



TECHNISCHE
UNIVERSITÄT
WIEN

BACHELOR'S THESIS

**Anti-Windup Observer Design for MIMO Systems
Applied to a Three-Tank Model**

AUTHOR: RAQUEL MARÍA CASAÑ CRESPO

ADVISOR: LUKAS BÖHLER

Academic Course: 2019-20

ABSTRACT

The problem of saturating inputs is a common issue in control engineering practice. Control algorithms with integration of the control error are often applied in industrial systems and the actuators of those systems are typically limited. For example, a motor has a minimum and a maximum torque he can be operated within. If the controller wants to exceed these physical limits over a longer period, so called Windup effects occur. These Windup effects can cause severe performance losses or even instability of the plant. The idea is to counter these effects with the implementation of Anti-Windup (AW) methods. While various approaches exist for single-input-single-output (SISO) systems, the task of Anti-Windup design becomes more complex for so called multi-input-multi-output (MIMO) systems.

The purpose of this Bachelor Thesis is to implement a state-of-the-art Anti-Windup observer-based design method from literature. The proposed design scheme shall be investigated based on a common three tank system and the performance of two controller, one with AW and one without, are to be compared.

TABLE OF CONTENTS

1.	Introduction. The Windup Problem	4
2.	The model	6
2.1.	State Space Models	6
2.2.	The three-tank system	7
2.3.	Observability and controllability	7
3.	Design of the controller	10
4.	Simulation with saturation of the actuators	12
4.1.	Simulation without Windup	12
4.1.1.	Simulation with a saturation of $20 \frac{cm^3}{s}$	13
4.1.2.	Simulation with a saturation of $15 \frac{cm^3}{s}$	14
4.1.3.	Comparison of outputs	16
4.1.4.	Control error when saturation is applied	16
4.2.	Simulation with Windup	17
5.	Design of the Anti-Windup Controller	20
5.1.	Computation of the observer matrix	20
5.1.1.	Method 1	21
5.1.2.	Method 2	22
5.2.	Implementation of the methods and comparison	22
5.2.1.	Simulation with a saturation of $25 \frac{cm^3}{s}$	24
5.2.2.	Simulation with a saturation of $60 \frac{cm^3}{s}$	25
6.	Conclusion and outlook	27
6.1.	Further Anti-Windup methods	27
6.2.	Summary of results	27

LIST OF FIGURES

Figure 1. The three-tank system [11]	7
Figure 2. Stability of the closed-loop represented in a pole-zero map	11
Figure 3. Comparison of the reference and the output of the system without having applied saturation with small reference changes	12
Figure 4. Plot of the input signal when no saturation is applied with small reference changes...	13
Figure 5. Comparison of the input signal with and without saturation. Example 1	14
Figure 6. Comparison of the reference and the output with saturation. Example 1	14
Figure 7. Comparison of the reference and the output with saturation. Example 2	15
Figure 8. Comparison of the input signal with and without saturation. Example 2	15
Figure 9. Comparison of the reference and outputs applying different saturations.....	16
Figure 10. Comparison of the control error and the step references when no saturation is applied.	17
Figure 11. Windup example. Comparison of the input with and without saturation.	18
Figure 12. Windup example. Comparison of the control error with and without saturation ...	19
Figure 13. Windup example. Comparison of the reference, the output without saturation and the output when saturation is applied.	19
Figure 14. Comparison of the reference and the output of the system having implemented an Anti-Windup observer using method 1. Example 1	23
Figure 15. Comparison of the reference and the output of the system having implemented an Anti-Windup observer using method 2. Example 1	23
Figure 16. Comparison of the reference and the output with and without Anti-Windup. Example 1.....	24
Figure 17. Comparison of the inputs with and without Anti-Windup. Example 1	24
Figure 18. Comparison of the inputs with and without Anti-Windup and without saturation. Example 1	25
Figure 19. Comparison of the reference and the output with and without Anti-Windup. Example 2.....	26
Figure 20. Comparison of the inputs with and without Anti-Windup. Example 2.....	26

1. Introduction - The Windup Problem

Windup is defined as the undesired behaviour a system shows when it has been designed in a way that ignores the effects of saturation leading to large oscillations and instability. It is caused by the combination of the integral action in the controller and the saturation of the actuators of the system [1, 3]. Given a system with a controller based on state vector feedback with integration of the control error, Windup provokes the rupture of the feedback loop, the system behaves as in open loop and the controller loses the function and purpose for which it was designed [4].

To understand this phenomenon, it is necessary to define the concept of saturation in this context. Actuator saturation materializes when a controller demands a signal that is beyond what the actuator can actually deliver [1]. For a control system with a wide range of operating conditions, it may happen that the control variable reaches the actuator limits [3]. All actuators have technological and physical limitations. Valves have a minimum and maximum aperture, pumps can achieve up to maximum pressure and power cables can admit up to a certain amount of current. For instance, giving the command (pressing a button in a device) to a speaker to turn music louder when it cannot admit more electrical current, will not make the sound more intense. The system now is saturated as the actuator has reached its limit and maximum performance. The coil that provokes the vibrations that are transformed into sound waves will not generate a bigger magnetic field than the produced by the maximum current that is actually going through the coil, without regard on how many times the button in the device is pressed.

Hence, there are situations where saturation is inevitable. When it takes place in a system where there is a controller with integration of the control error to remove the steady state error, Windup problems appear. The systems designed should be prepared to deal with large references that they cannot fulfil and saturations leading to Windup. It must be guaranteed that the controlled systems behave coherently, even if due to their limitations they will never reach the reference the controller aims to achieve [6].

To illustrate how Windup appears, suppose a system with a certain limitation of the actuator. Once the input command reaches the saturation limit, the actuator will not be able to increase its performance, it will work at a maximum constant value. Nevertheless, there is still control error, as the system is not fulfilling the reference input, and it is not going to be able to reach it. Hence, the integral error keeps increasing while the actuators work at full capacity while they receive orders of increasing its performance, without being able to do it. This is what we call Integral Windup. The authentic problem materializes when there is a change in the reference to a lower value. The error starts decreasing and the controller should decrease the value of the actuator. It will do so from a very high value as the error had been increasing all the time the actuators were saturated (this is what we have called Integral Windup) and so the controller command will actually begin to decrease but it will do so from a such a high value that a delayed response of the system is obtained. Until the controller commands return to values that are below saturation limits, the output remains unchanged [2, 3, 4].

The straight-forward solution could seem to provide the system with actuators powerful enough to never reach saturation for a certain application. This solution is not practical nor economically

and technologically feasible in most industrial applications [1]. It would mean large, expensive and energy consuming actuators for systems that do not need such complexity at most of its operating time and applications. Also, even if very powerful actuators were implemented, it cannot be totally assured that extraordinarily large signals will not punctually appear, causing an undesired response. Anti-Windup is the most effective and efficient way of preventing this phenomenon.

Anti-Windup systems are meant to reduce the time that it takes to reverse the Integral Windup. This Bachelor's thesis will be focused on implementing a type of Anti-Windup that modifies the controller equation and not the system itself [2].

According to [6] the Anti-Windup methods can be classified in two groups. First, in the one-step approach, a controller is designed from the ground up considering both the saturation constraints and the closed loop performance. This approach has been widely used and studied but it is criticized because its design it is not intuitive and it is not always applicable.

In this thesis, the second approach is to be developed. The objective is to add a separation to the controller that will be called Anti-Windup observer, addressed to handle the constraints. It intervenes only when there is saturation modifying the closed loop. Otherwise, the controller works as if no Anti-Windup was implemented. One important advantage of this approach is that it can be implemented in existing controllers that have a very good performance in certain applications but have an awful performance in presence of actuator saturation [6].

2. The model

2.1. State space models

The implementation of the Anti-Windup system in this thesis is applied to a state space model MIMO based on a three-tank system. MIMO models make the Windup problem more complex but also allow accurate representations of real dynamic systems. MIMO state-space models are defined as systems with multiple inputs and multiple outputs (instead of one input and one output as in the so-called SISO systems) that use a set of internal variables known as state variables to mathematically describe a physical system by a set of first-order differential equations. [8, 7].

The continuous-time state-space equations for the state-space models are:

$$\dot{x} = Ax + Bu + Ez; \quad x(t_0) = x_0 \quad (2.1)$$

$$y = Cx + Du + Fz \quad (2.2)$$

Where y is the output vector, x the state vector and u the actuator vector. The output vector represents the variables of interest. Also, the actuator vector is significant in this thesis because is the variable to which saturation will be applied. Furthermore, the state vector contains the state variables, which are the minimum set of variables that describe the system completely. The variable z is the disturbance vector [7, 9]. Disturbances are not considered in this thesis because it is going to focus on the Windup problem originated by the reference input. This results in:

$$\dot{x} = Ax + Bu; \quad x(t_0) = x_0 \quad (2.3)$$

$$y = Cx + Du \quad (2.4)$$

Where A is the system matrix and B is the input matrix. Both are determined by the structure and properties of the system. On the other hand, C is the output matrix and D is the feedthrough matrix. These matrices depend on the choice of output variables [3, 9].

Unlike other model representations based on an input-output description of the system, state space models allow to work with MIMO systems and to understand models and simulations in a deeper way. As the representation is done using ordinary differential equations, the way the system changes in an instant of time is function of the current state of the system in that moment and the input vector. However, the most important advantage that state-space representation draws is that all the considered states of the system are represented, and the internal variables of the plant can be tracked at all time providing information of the internal structure of the system and its dynamics. [7, 9, 10].

2.2. The three-tank system

To illustrate the effects of saturation of the actuators, Windup effects, and the change in behaviour when Anti-Windup is implemented, different reference steps are applied in the following chapters to a three-tank system model. An approximate scheme of this system is represented in Figure 1.

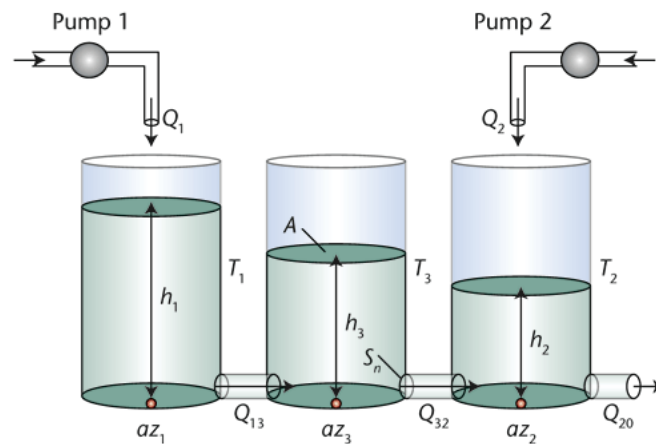


Figure 1. The three-tank system [11].

The key elements of this system are three interconnected tanks and two pumps. The actuator vector consists on the command values Q_1 and Q_2 . These are the fluid volume flows provided by pumps 1 and 2. On the other hand, the state vector is composed by the height level of the three tanks although only two of the three heights can be controlled, the height of fluid in tanks 1 and 2 (h_1 and h_2 respectively). These two controlled heights form the output vector. The initial values for these variables are 24 cm and 35 cm, respectively. The model is linearized around this point, the operating point.

The behaviour of each pump and the fluid height in each tank will directly influence the behaviour of the other elements in the system as they are all interconnected.

2.3. Controllability and observability

In chapter 3 a controller for the system will be designed. Later, in chapter 5, modifications based on an observer model will be applied to this controller to tackle the Anti-Windup problem. For this controller and its posterior modification to work, two important concepts are to be checked: the controllability and the observability of the system.

Controllability determines whether from an initial state, each state variable, and each combination of state variables in the system is possible in a finite time employing the inputs. [12, 13, 14]. This concept is defined in [7] as:

“The LTI (Linear Time Invariant)-MIMO system

$$\dot{x} = Ax + Bu; x(t_0) = x_0 \quad (2.5)$$

is called completely state controllable if by an appropriate choice of the unconstrained control vector $u(t)$ in a finite time interval $t_0 \leq t \leq t_1$ each initial state $x(t_0)$ can be converted into any state $x(t_1)$.”

The state controllability depends on the matrices A and B and can be studied through two criterions defined in [7]. Being n the length of the matrix A :

The Kalman controllability criterion states that the system (2.5) is fully state controllable if:

$$\text{rank} ([B \ AB \ A^2B \ \dots \ A^{n-1}B]) = n \quad (2.6)$$

The Hautus controllability criterion states that the system (2.5) can be completely controlled if it is fulfilled that:

$$\text{rank} ([\lambda_i I - A \ B]) = n \quad (2.7)$$

Where λ_i are all the eigenvalues of the matrix A , being $i = 1, 2, \dots, n$.

On the other hand, observability determines whether there is enough information in the measurements so that each state in the state vector can be known from the outputs [12, 13, 14]. In a more formal way, observability is defined in [7] as:

“The LTI multivariable system

$$\dot{x} = Ax + Bu; x(t_0); x(t_0) = x_0 \quad (2.8)$$

$$y = Cx + Du \quad (2.9)$$

is called fully state observable if from the knowledge of the input $u(t)$ and the output $y(t)$ in a finite time interval $t_0 \leq t \leq t_1$ each initial state x_0 can be uniquely determined.”

It depends on the state matrix A and the output matrix C . Also, two criterions defined in [7] can be applied here:

According to the Kalman observability criterion, the system (2.8) and (2.9) is only fully observable if:

$$\text{rank} \left(\begin{bmatrix} C \\ CA \\ \vdots \\ CA^{n-1} \end{bmatrix} \right) = n \quad (2.10)$$

The Hautus observability criterion guarantees that the system (2.8) is fully observable if the condition:

$$\text{rank} \left(\begin{bmatrix} \lambda_i - A \\ C \end{bmatrix} \right) = n \quad (2.11)$$

Is true for all the eigenvalues λ_i ($i = 1, 2, \dots, n$) of the matrix A .

If both observability and controllability are fulfilled, the system can be handled with feedback and observer controllers. It can be assured that with the right design the system will be able to reach a stable steady-state. Otherwise, despite an extraordinary effort to design an effective controller, the system would not respond as desired.

3. Design of the controller

Before tackling the Windup problem, a feedback controller with integration of the control error is designed [7]. Pole placement is the method used to implement this controller and achieve stability of the three-tank system. The poles of the original system are defined by the eigenvalues of the matrix A in (2.1), that contains the information about the dynamics of the system, and their location determines the stability of the plant. In order to move the poles to a location where the system becomes stable, pole placement is used [15]. Through this method, a gain matrix K' is obtained and used to compute a new state matrix A' , with different eigenvalues than the original state matrix that represents the new system matrix with the defined poles for the closed-loop system after implementing the controller. It is obtained:

$$A' = A - BK' \quad (3.1)$$

To work with this approach and design the controller, it is needed to work with the extended state equations. Firstly, the state equations defined in the previous chapter, without considering disturbances are:

$$\dot{x} = Ax + Bu; \quad x(t_0) = x_0 \quad (3.2)$$

$$y = Cx + Du \quad (3.3)$$

Secondly, a new variable is introduced:

$$p(t) = \int_0^t ((y(\tau) - w(\tau))d\tau \quad (3.4)$$

It can also be defined as:

$$p(t) = y(t) - w(t) = Cx + Du - w \quad (3.5)$$

Where w is the reference input to the controller and u the input to the plant. With the state-space equations and the new variable p , the extended state equation is constructed as:

$$\dot{s} = \begin{bmatrix} A & 0 \\ c^T & 0 \end{bmatrix} s + \begin{bmatrix} b \\ 0 \end{bmatrix} v \quad (3.6)$$

Where:

$$s = \begin{bmatrix} s_1 \\ s_2 \end{bmatrix} = \begin{bmatrix} x - x_s \\ p - p_s \end{bmatrix} \quad (3.7)$$

$$v = u - u_s \quad (3.8)$$

$$\dot{s} = \begin{bmatrix} \dot{x} \\ \dot{p} \end{bmatrix} \quad (3.9)$$

Applying pole placement to the extended equations of the system, a matrix K is obtained. It can be decomposed in two matrices:

$$K = [K_T \quad K_w] \quad (3.10)$$

The matrix K_T is the scaling term for the steady state error and is composed by the first columns of the matrix K . The number of columns depends on the dimension of the state vector x . This means, the number of columns of K_T must match the number of states. The remaining columns of the matrix K compose the matrix K_w , which is the gain matrix.

With these two matrices and introducing an integrator, the following control law is obtained:

$$u = -K \begin{bmatrix} x \\ p \end{bmatrix} = -K_T x + K_w \int_0^t (w - y) dt \quad (3.11)$$

The closed loop continuous-time state-space model that is obtained and to which saturation will be applied is represented by the following equations:

$$\dot{x} = A - BK_T x + BK_w w \quad (3.12)$$

$$y = C - DK_T x + DK_w w \quad (3.13)$$

In this case, to assure closed-loop stability it is necessary that the eigenvalues of $A - BK_T$ are placed in the left-half plane. In Figure 2 poles are marked by x and it is shown that all of them are located in the stability region.

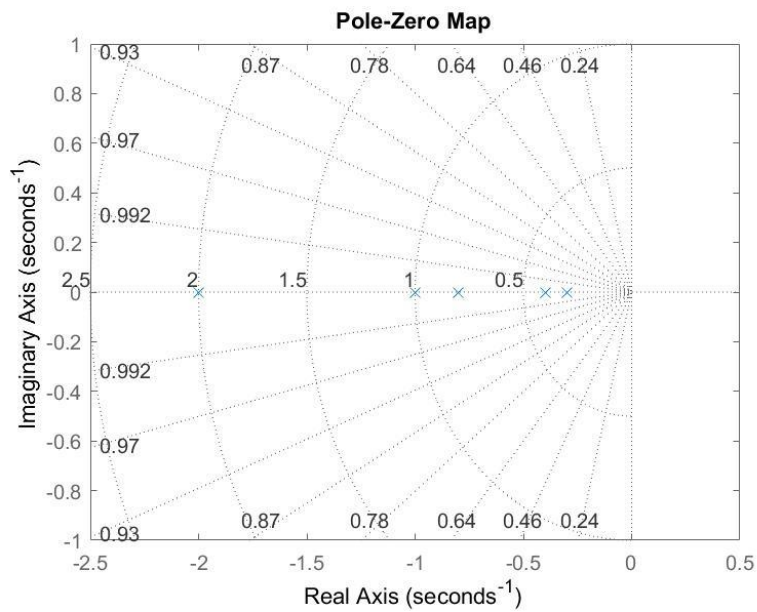


Figure 2. Stability of the closed-loop represented in a pole-zero map.

4. Simulation with saturation of the actuators

In this chapter the controller designed in the previous chapter will be implemented to the system, obtaining a closed-loop feedback system, and saturation will be applied to the actuators. The aim of this chapter is to analyse the effect of different saturations in the system with a feedback controller before and after Windup appears.

4.1. Simulation without Windup

The initial heights of tanks are 24 and 35 cm, being $h_0 = [24 \ 35]$ cm. The changes in the reference in this chapter will be the same in all plots. From the operating point the reference signal increases these heights by $1.2 \cdot h_0$, then decreases to the $0.8 \cdot h_0$ value and then returns to the initial value. First, without having applied saturation, the changes in the level of the water in the first and second tanks respectively can be observed in Figure 3. It is represented the fluid height level in Tank 1 and Tank 2 respectively for 160 seconds of simulation, facing the small changes in the reference described above.

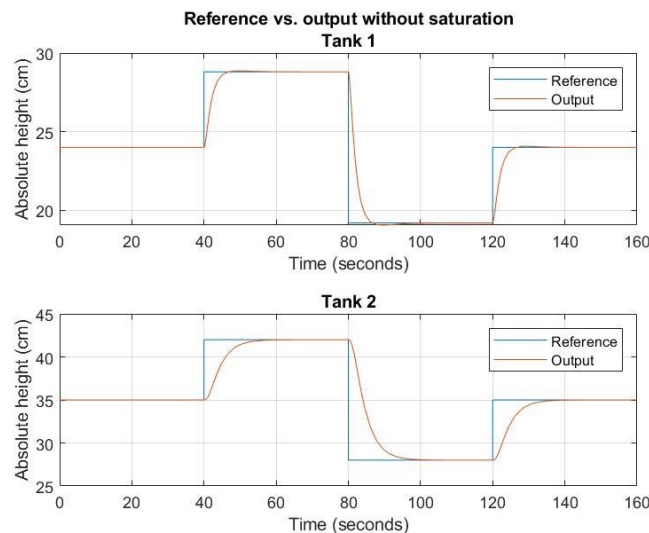


Figure 3. Comparison of the reference and the output of the system without having applied saturation with small reference changes.

With the designed controller and without saturation, references are smoothly reached by the system in a short span of time. On the other hand, in Figure 4 it can be observed that the actuator signal u has no restrictions, the actuators operate without limitations. They work until the output matches the reference. When this happens the signal turns zero and the actuators stop. In this modelled system, the actuator 2 has to keep acting at some points at a constant level to maintain the desired height, while the actuator 1 stops. In this simulation, where no saturation has been applied yet, the actuators rise up to the value that is needed to achieve the reference and this is why good results are obtained in the output. It should be noted that the negative values that can be observed in Figure 4 are not physically possible. They correspond to the assumed hypothesis that the pumps could subtract flow from the system.

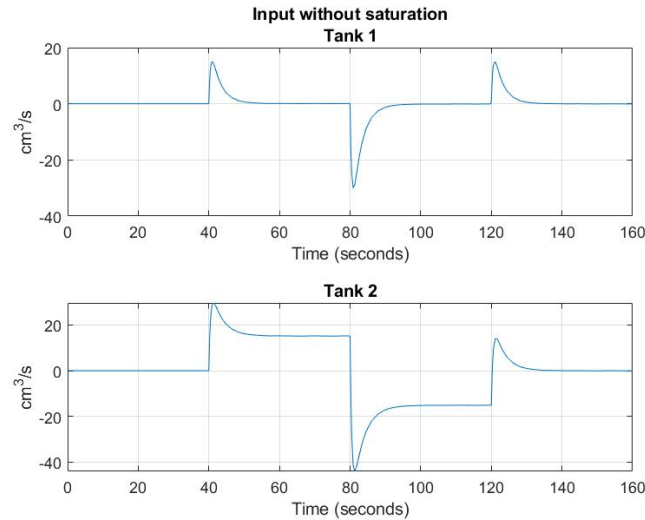


Figure 4. Plot of the input signal when no saturation is applied with small reference changes.

4.1.1. Simulation with a saturation of $20 \frac{cm^3}{s}$.

In this chapter, saturation to the input is applied. The volumetric flow the pumps can provide has been limited to -20 and $20 \frac{cm^3}{s}$. As in the previous section was stated, the negative values are not possible and, in this chapter, have been represented in absolute values so that the minimum value that they reach is zero. The input to the three-tank system (the actuator vector u) is plotted in Figure 5. A comparison between the input with and without saturation has been made to illustrate the effect saturation has on the performance of the actuators. It is in contrast to what the pumps should be delivering so that the system worked properly, and what they actually provide due to their limitation. Instead of an input command that stops after a short period of time, it can be observed that, when compared to the input without saturation, the saturated one stays at a constant value for a longer time until the reference is reached by the output.

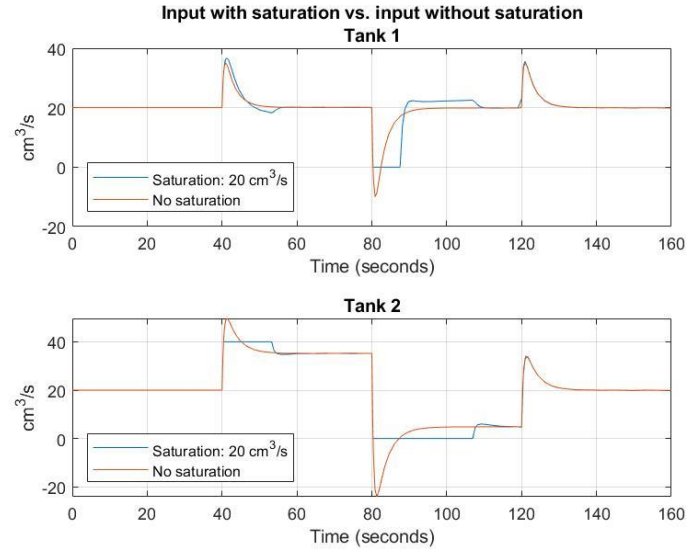


Figure 5. Comparison of the input signal with and without saturation. Example 1.

On the other hand, the effects of saturation in the output can be appreciated in Figure 6. References are reached by the output but they do so in a big span of time and it presents unnatural oscillations.

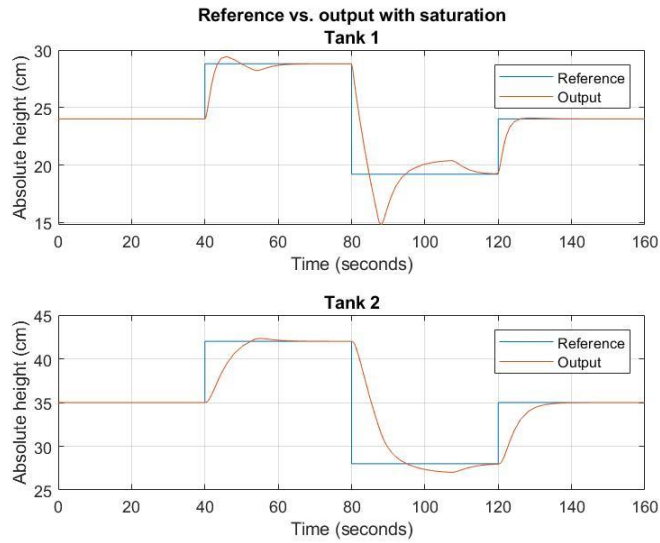


Figure 6. Comparison of the reference and the output with saturation. Example 1.

4.1.2 Simulation with a saturation of $15 \frac{cm^3}{s}$

The behaviour of the system and the stability become worse while the input saturation increases. A saturation of $15 \frac{cm^3}{s}$ is applied to illustrate how, while the performance span of the actuators is smaller, the oscillations and instability become bigger. In Figure 6 it can be observed that the peaks in the output before reaching the reference are bigger than in the previous plot where a saturation of $20 \frac{cm^3}{s}$ was applied. Although in general the behaviour follows the same pattern in both cases, more saturation however leads to worse results in the output and in more unstable input commands as is illustrated in the Figures 7 and 8.

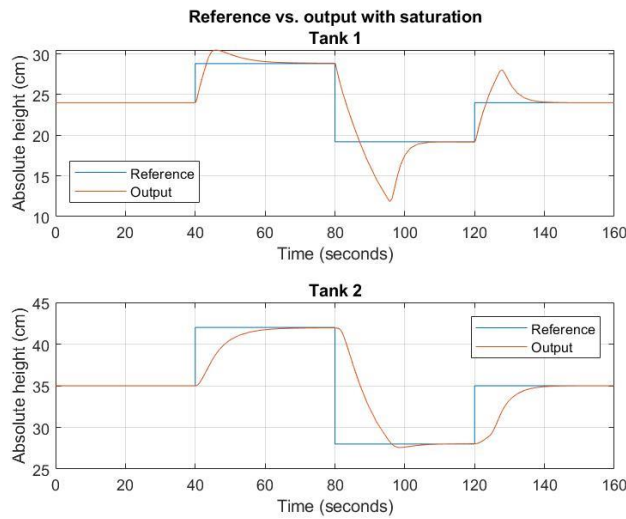


Figure 7. Comparison of the reference and the output with saturation. Example 2.

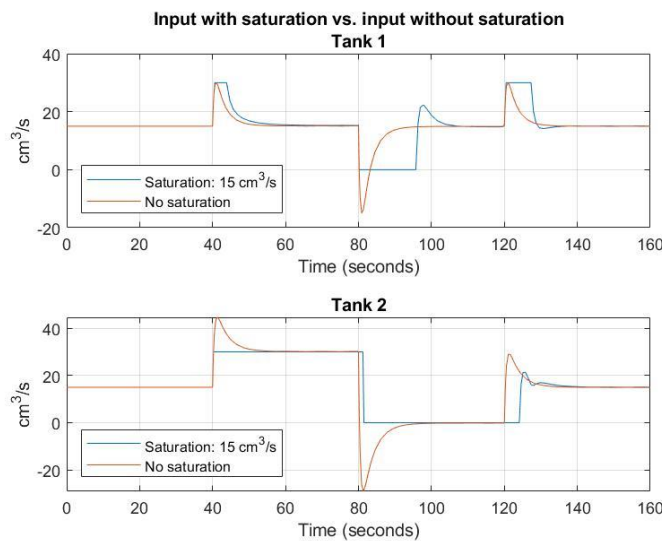


Figure 8. Comparison of the input signal with and without saturation. Example 2.

4.1.3. Comparison of outputs

To sum this up, Figure 9 presents a comparison of the different outputs obtained in the different situations and the reference the controller aims to reach. In all cases the reference is reached within 40 seconds (this would not happen if Windup effects appeared) but the oscillation and the settling time are greater as the saturation is increased. The system would become even more oscillating and unstable if we kept on reducing the performance of the actuators until Windup effects appeared. This will happen whenever the actuators have no longer the capability of reaching at least one of the references due to an incompatibility between the value that is to be reached and a too low performance of the actuators.

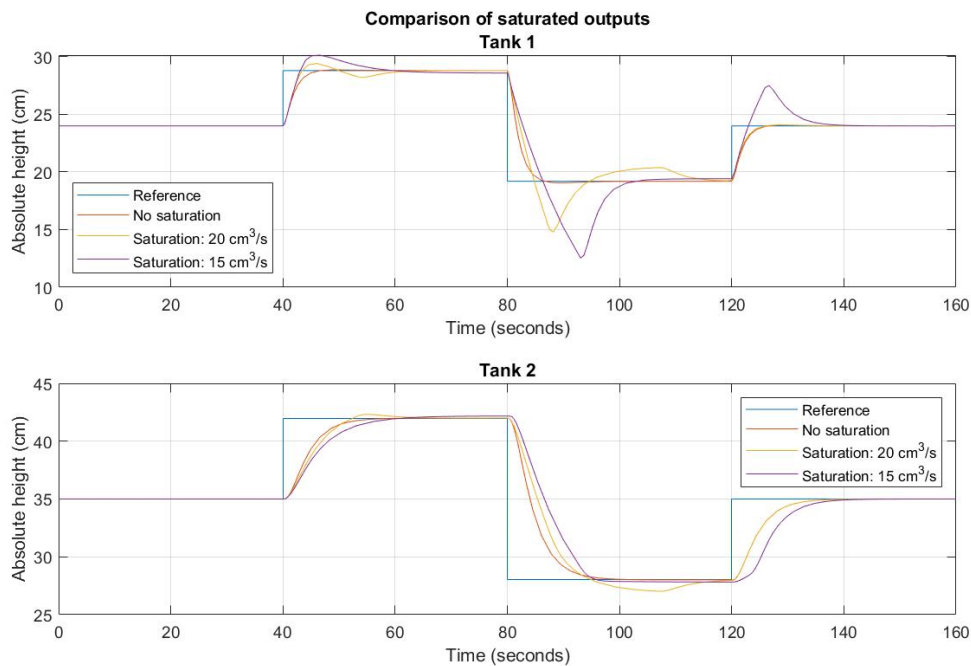


Figure 9. Comparison of the reference and outputs applying different saturations.

4.1.4. Control error when saturation is applied

The control error is the difference between the output and the reference at every time. It is important to study it, as it plays an important role in the undesired behaviour of the system with saturation. The objective of the controller is setting the control error to 0. Whenever this happens, it means that the reference input and the final output are the same. Nevertheless, when the control error is different from zero the actuators will receive orders of increasing its performance, eventually leading to Integral Windup. Two cases are evaluated in Figure 10: the control error when the system is saturated and when it is not.

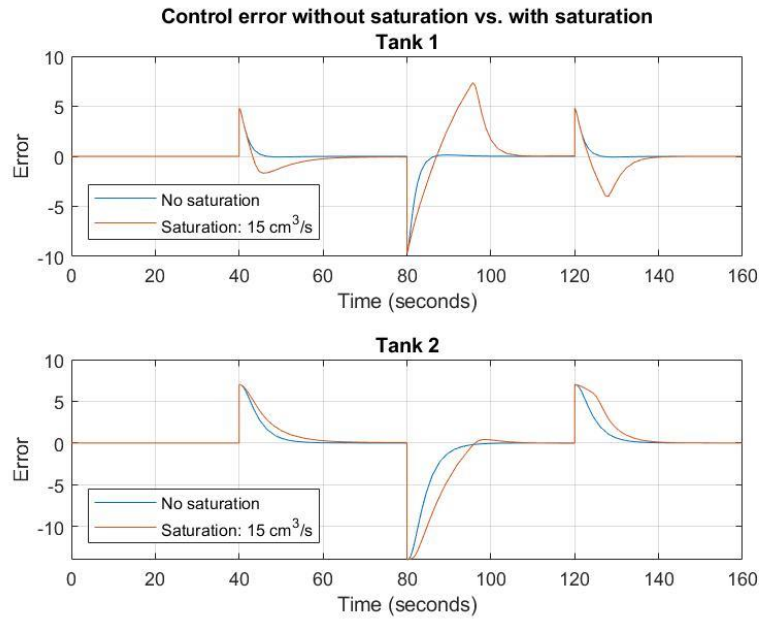


Figure 10. Comparison of the control error with and without saturation.

It can be noticed that in both cases for the reference used in this chapter, after each step, there is a certain control error that decreases after a few seconds, eventually getting to 0. In the case where no saturation occurs, the control error disappears after a short time, the settling time in the output is short and no overshoots emerge. In the case when saturation occurs, the control error also gets to 0 eventually but, unlike the non-saturated one, it is greater and it oscillates more as a consequence of this saturation. The system also needs more time to get to the point where reference and output match.

4.2. Simulation with Windup

So that Windup effects can be observed, the references have to be big enough so that the actuators of the system do not have the capability of delivering an outcome that reaches them. In the previous simulations saturation was applied to the system but Windup effects could not be appreciated because the reference steps were small and the actuators were still capable of achieving the desired output despite oscillation. The reference signal used in this part is bigger than the used before. The reference increases the initial heights in 24 and 35 cm, then, from that point, decreases the tank heights in 48 cm and 70 cm, respectively (emptying the tanks) and then returns to the initial value.

It is important to highlight that the lower input saturation in all cases in this chapter is limited to $-18 \text{ cm}^3/\text{s}$ to make the analysis physically feasible. Also, in order to simplify the study of the system, negative values in the input mean that the pumps would be able to subtract fluid from

the tanks. Also, the input and output plots are all expressed in means of absolute values. An input saturation of 25 cm³/s is now applied. The input value is significantly shortened with the saturation applied compared to what the system demanded without saturation as showed in Figure 11. This difference can be specially appreciated in the second 200. At this point as well as in the second 400, the input ignores the fact that there has been a step change in the reference and stays at its maximum value for longer than it should be.

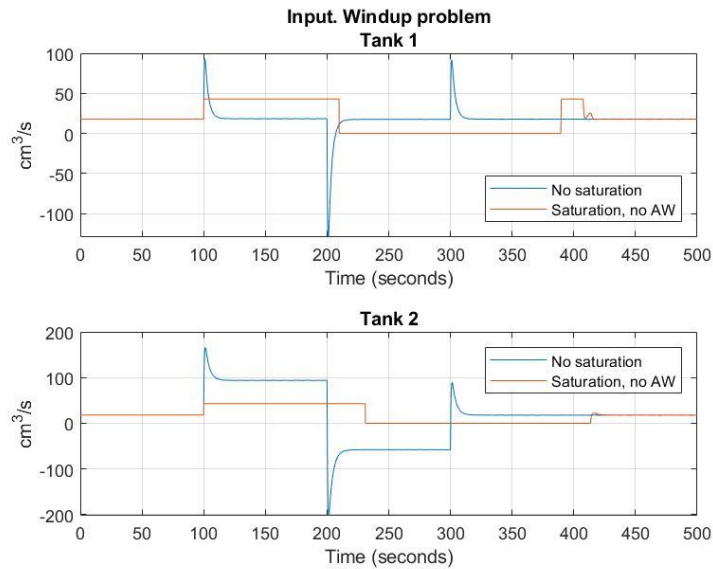


Figure 11. Windup example. Comparison of the input with and without saturation.

The behaviour of the input is a consequence of the control error. Windup appears because of the interaction of the saturation in the actuators and the integral action in the controller. Once the actuators arrive to their saturation limit, they perform at a maximum constant value. Nevertheless, as it can be observed in Figure 12 that the control error keeps increasing. This means that the actuators are asked to increase its performance without being able to do it. When the reference changes to a lower value, the control error starts decreasing but it does so from such from a value over zero so the actuators do not receive the order of decreasing their value until the control error is below zero. For instance, the value of the first step reference between 100 and 200 seconds is the most representative. It can be observed in Figure 12 that for the second reference the control error never reaches zero so, when there is a change in the step reference at 200 seconds, the control error decreases from a value superior from zero and that is the reason why the response is delayed.

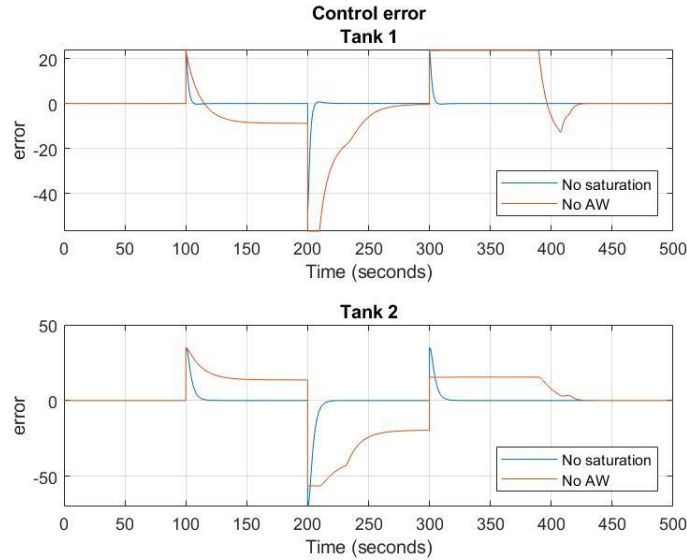


Figure 12. Windup example. Comparison of the control error with and without saturation.

In Figure 13 the output of the system is represented. In this plot Windup effects can be appreciated. Anti-Windup has not been implemented yet. It can be noticed how the system response is slow, changing its behaviour few seconds after the reference has changed. Also, it is observed that in the upper plot, the output surpasses the reference and in the lower side, reference cannot be reached. The system tries to reach both references but is not able to due to the actuator restrictions. While trying to reach the second reference, the tank 1 receives too much fluid from the pump and still it is not enough to reach the second reference in tank 2. Hence, the state of each tank conditions the behaviour of the other.

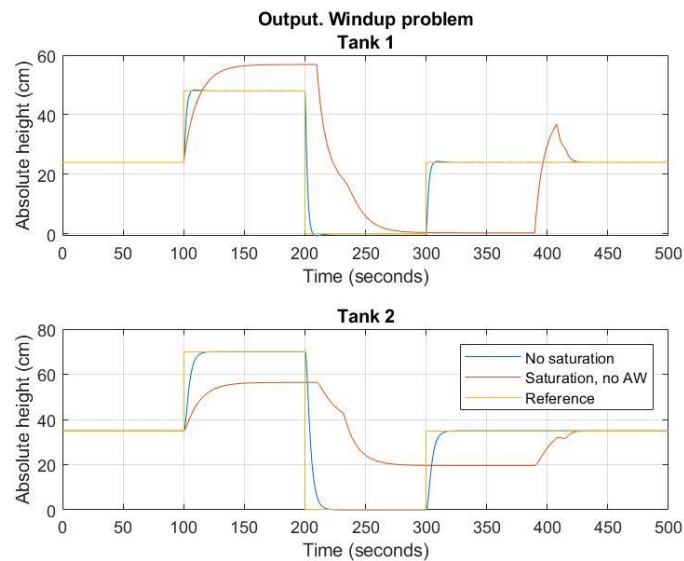


Figure 13. Windup example 1. Comparison of the reference, the output without saturation and the output when saturation is applied.

5. Design of the Anti-Windup controller

To avoid the behaviour shown in chapter 4.2. in this chapter Anti-Windup system is going to be designed and its effectivity will be tested and compared.

5.1. Computation of the Observer Matrix

The Anti-Windup controller that is to be designed is the result of the modification of the closed-loop equations obtained after implementing the controller designed in chapter 3. As a result, an observer-based controller is obtained. This is a dynamic feedback controller where the so-called observer of the system estimates the state space variables of the controlled system based on the measured outputs and the known inputs. This estimate is used by the feedback controller as if it were the actual state of the system. This way, observers reconstruct variables that are not accessible or cannot be measured [12, 16].

From the extended state equation (3.6) it can be defined:

$$A_{ext} = \begin{bmatrix} A & 0 \\ C^T & 0 \end{bmatrix} \quad (5.1)$$

$$B_{ext} = \begin{bmatrix} B \\ 0 \end{bmatrix} \quad (5.2)$$

The differential equations representing the closed loop once the feedback controller designed in Chapter 3 is implemented can be expressed as:

$$\dot{x}_c = A_c x_c + B_c e \quad (5.3)$$

$$u = C_c x_c + D_c e \quad (5.4)$$

"e represents a combination of plant measurements and reference signals" [17].

$$A_c = A_{ext} - B_{ext}K \quad (5.5)$$

The matrix K was calculated in Chapter 3.

$$B_c = \begin{bmatrix} 0 & 0 \\ 0 & 0 \\ 0 & 0 \\ -1 & 0 \\ 0 & -1 \end{bmatrix} \quad (5.6)$$

$$C_c = [C \quad 0] \quad (5.7)$$

$$D_c = D \quad (5.8)$$

Based on [17], a modification to the previous closed loop equation is done to add an Anti-Windup observer L such that:

$$\dot{x}_c = A_c x_c + B_c e + L[sat(u) - u] \quad (5.9)$$

$$u = C_c x_c + D_c e \quad (5.10)$$

Where u represents the input that the controller demands and $sat(u)$ the saturated input that the actuator actually delivers. As exposed in the introduction, the objective is to add a separation to the controller that will be called Anti-Windup observer, not changing the designed controller itself but adding a term on the equation of its closed loop. An advantage about this approach is

that the matrix gain L is external to the system. If saturation does not occur the terms $\text{sat}(u)$ and u have the same value and L will not change the controlled closed loop. To calculate the matrix L two methods are used based in [14].

5.1.1. Method 1

To obtain the matrix L , an algorithm exposed in [14] is implemented. With this method L' is calculated. L is a part of this matrix L' :

$$L' = -T_2^{-1}T_1B_{ext} \quad (5.11)$$

It is based on the assumption that the real matrices T and H exist and fulfil the following expression:

$$TA_{cl} = HT \quad (5.12)$$

To obtain T_1 and T_2 , first it is needed to compose T . To do that, A_{cl} is defined as:

$$A_{cl} = \begin{bmatrix} A_{ext} + B_{ext}D_cC_{ext} & B_{ext}C_c \\ B_cC_{ext} & A_c \end{bmatrix} \quad (5.13)$$

Being the matrices with the sub-index c the corresponding to the closed loop with the designed feedback controller, and the matrices with the sub-index ext the corresponding to the extended equation, already defined in (5.1), (5.2), (5.5), (5.6), (5.7) and (5.8). The Jordan decomposition of A_{cl} is used to obtain a matrix U that will be used to calculate the matrix T :

$$A_{cl} = U\Lambda U^{-1} \quad (5.14)$$

It is stated in [14] that the last n_c columns of T must have full rank and that "if U^{-1} is invertible, then T can be chosen as the last n_c rows of U^{-1} , i.e.,

$$T = [0 \ I]U^{-1} \quad (5.15)$$

where I is an $n_c \times n_c$ identity matrix." When this operation is done, T appears as:

$$T = [T_1 \ T_2] \quad (5.16)$$

The last n_c columns of T with full rank are named T_2 and the remaining columns, T_1 .

The problem one faces when implementing this method is choosing the value of n_c , i.e. the dimension of the identity matrix used to calculate T . To address the problem, n_c has been chosen as the length of the extended matrix A_{ext} . When this is done, T can be obtained as:

$$T = \begin{bmatrix} 0 & 0 \\ 0 & I \end{bmatrix} U^{-1} \quad (5.17)$$

And T_1 and T_2 can be extracted from the matrix T calculated with 5.17

$$T = \begin{bmatrix} 0 & 0 \\ T_1 & T_2 \end{bmatrix} \quad (5.18)$$

Now L' can be calculated as:

$$L' = -T_2^{-1}T_1B_{ext} \quad (5.19)$$

The matrix B_{ext} has been already defined in (5.2) and has dimensions $n \times k$. Being n equal to the length of A_{ext} and k equal to the number of controlled variables. Both matrices T_2 and T_1 are square matrices of dimensions $n \times n$. The matrix L is composed by the last k lines of the matrix L' .

5.1.2. Method 2

This second approach is simpler but proved to be as efficient as the previous one. This approach focuses on locating the eigenvalues of the state closed loop matrix (5.5) in a location where the system becomes stable, using pole placement. In chapter 3 it was used the same method to design the feedback controller with integration of the control error. The poles of the original state matrix were displaced using a gain matrix K . In this case, the matrix gain used to modify the eigenvalues of the closed-loop state matrix is named L' . As in Method 1, the last k columns of L' are selected and assemble the observer matrix L .

The question that arises in this method is where to place the poles of the system. The new observer poles must be faster than the closed-loop original poles. The new observer poles must be at least 10 times faster than the original ones. Most times it is enough to put the new poles in that location. The observer poles that are displaced correspond with the last k eigenvalues of the closed-loop state matrix, the rest of poles stay the same.

5.2. Implementation of the methods and comparison

In chapter 3 saturations of $25 \frac{cm^3}{s}$ and $60 \frac{cm^3}{s}$ were applied to the actuators and the Windup effects could be observed. For the same step references and time of simulation, both Anti-Windup methods are tested for each of the saturation values.

5.2.1. Simulation with a saturation of $25 \frac{cm^3}{s}$

First, the new controller is tested with the $25 \frac{cm^3}{s}$ actuator saturation. The output results can be seen in Figures 14 and 15. In both cases, the reference cannot be reached due to the limitations in the actuators. Nevertheless, Windup effects have disappeared. The response is smooth and not delayed, there are no oscillations and the references are reached when possible.

After the implementation of the Anti-Windup with both Method 1 and Method 2, the height level in tank 1 is almost the desired while the height level in tank 2 is far from the reference. Method 2 obtains slightly better results than Method 1. This difference is not significant although the output gets closer to the reference with Method 2. Despite this, the objective of the Windup is accomplished because the behaviour of the system has been corrected. It is not

unstable even if the references cannot be reached due to the technological limitations of the system.

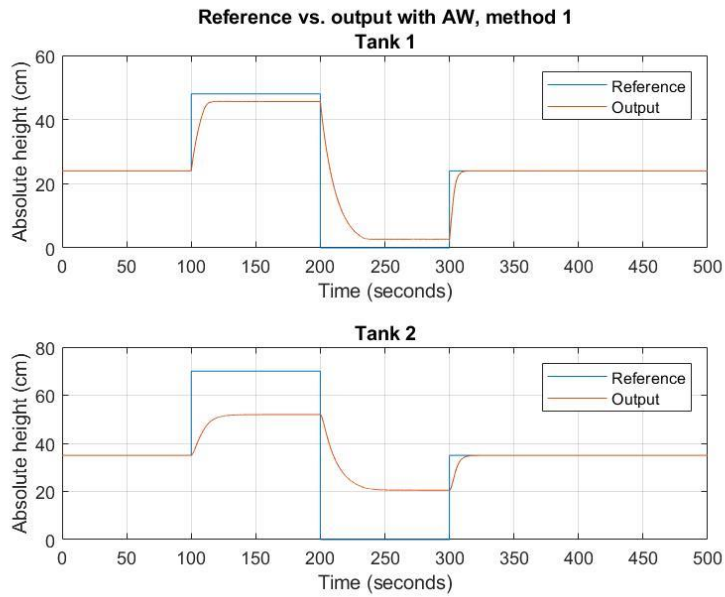


Figure 14. Comparison of the reference and the output of the system having implemented and Anti-Windup observer using method 1. Example 1.

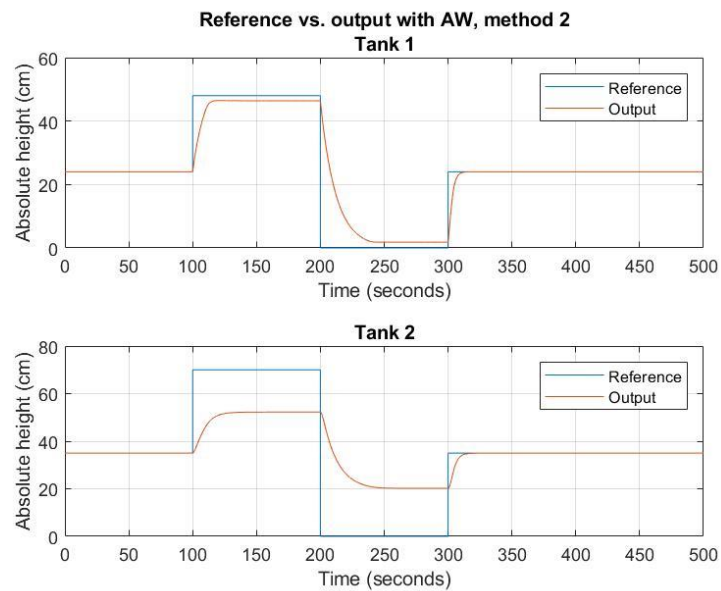


Figure 15. Comparison of the reference and the output of the system having implemented an Anti-Windup observer using method 2. Example 1.

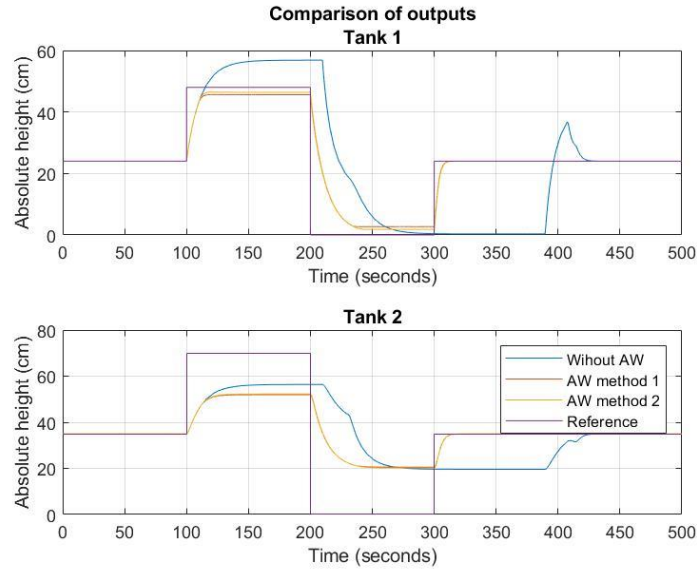


Figure 16. Comparison of the reference and the output with and without Anti- Windup. Example 1.

On the other hand, Anti-Windup also drives an important change of behaviour in the input. All signals are saturated, but in Figure 17 a perfectly timed response of the actuators can be observed. In contrast, when Anti-Windup is not implemented a extremely delayed response of the actuators can be observed. Also, when Anti-Windup is used signal oscillations, such as the one between the seconds 400 and 450, disappear. Moreover, both methods result in almost identical input signals although the Method 2 shows a slightly better response in the input in the second 300 with no oscillation.

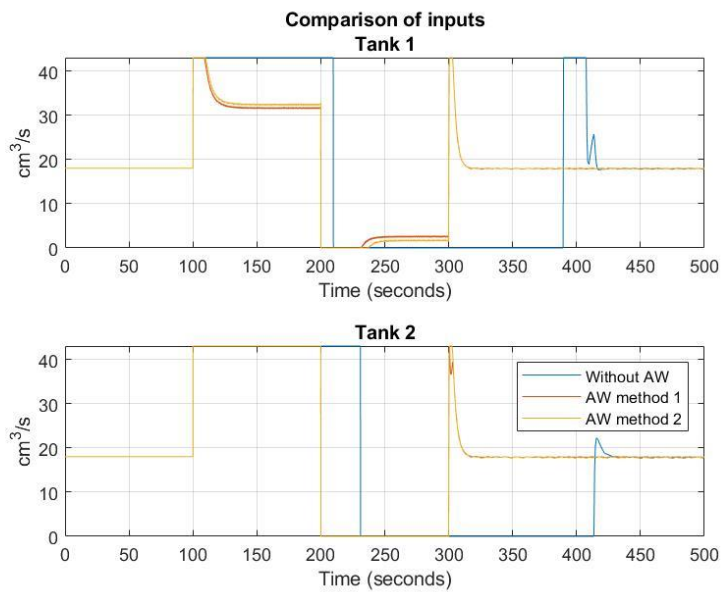


Figure 17. Comparison of the inputs with and without Anti-Windup. Example 1

When compared to the input without saturation, the constraints of the actuators and the importance of Anti-Windup systems can be observed. In Figure 18 it can be appreciated the huge difference between what the system would need that the actuators provided to reach the reference and what they actually provide.

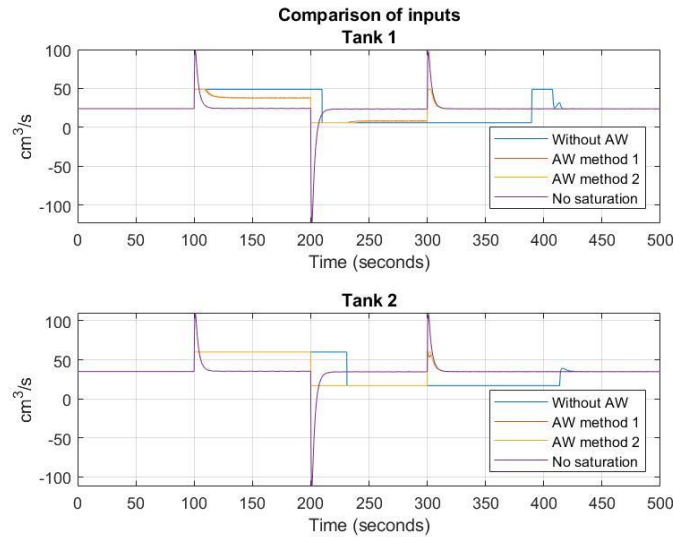


Figure 18. Comparison of the inputs with and without Anti-Windup and without saturation.
Example 1

5.2.2. Simulation with a saturation of $60 \frac{cm^3}{s}$.

In order to illustrate with another example the performance of the Anti-Windup systems, a saturation of $60 \frac{cm^3}{s}$ is applied to the actuators. The output in this case is closer to the reference than in the previous example as the actuators have a higher performance. Also, the Anti-Windup corrects the behaviour of the system, obtaining results almost as good as the desired ones and providing a smooth response.

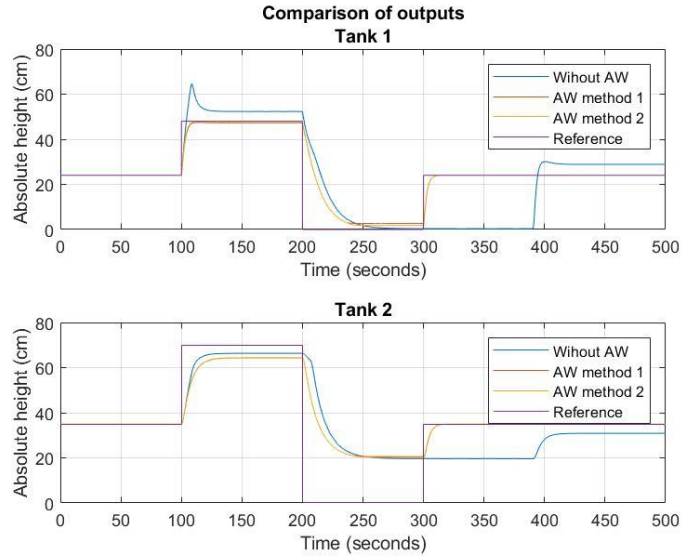


Figure 19. Comparison of the reference and the output with and without Anti-Windup. Example 2

Also, as it happened with the case where actuators were limited to $25 \frac{cm^3}{s}$ the results obtained with each of the methods are very similar both in the output and the input signals. In this case there is not even a visible difference in the input signal between the two of the methods.

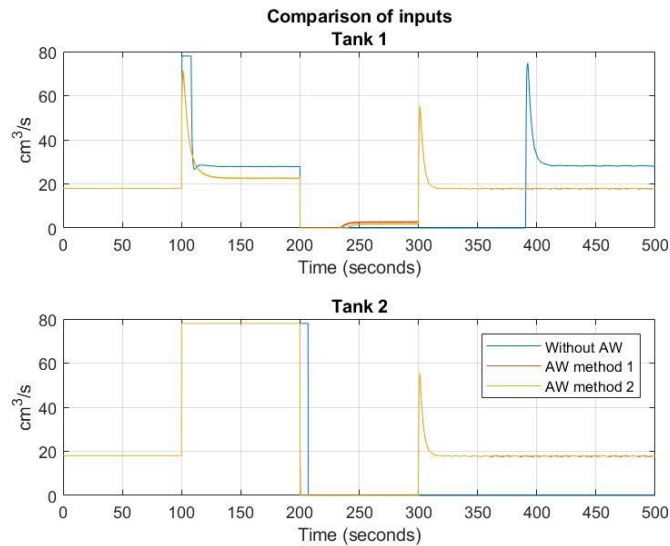


Figure 20. Comparison of the inputs with and without Anti-Windup. Example 2

6. Conclusion and outlook

6.1. Further Anti-Windup methods

Looking ahead to the future of Anti-Windup methods, they are still in research and there are many questions unanswered and unproved theories. New procedures are being developed. Most known time-invariant Anti-Windup methods have been based in first, designing a controller without considering the possible nonlinearities caused by the actuators' saturation, and then implementing a compensator that minimizes the adverse consequences caused by the emerging Windup [18, 19]. A theory based in this principle has been developed in this thesis. Nevertheless, in [19] and [20] recent methods that allow to design a state feedback controller and to implement the windup compensator simultaneously is proposed. These methods are based on TS-fuzzy models using the Lyapunov theory. Moreover, an Anti-Windup structure based in MFC (model-following control) has been developed in [21] showing robust results.

Also, most anti-windup strategies are based on integration (the integral action turns off when saturation occurs), calculation scheme (where the integral action is reduced in magnitude when the output reaches saturation) or a combination of the previous. Another strategy, is the one that uses the stochastic arithmetic. It is not widely used but in [22], where the Anti-Windup procedure is based in Field Programmable Gate Arrays (FPGA), stochastic arithmetic is useful to provide an effective outcome as the FPGA have got poor calculation ability [22].

6.2. Summary of the results

In the present Bachelor's Thesis, the study of the Windup effect and the implementation of Anti-Windup schemes applied to a three-tank system has been done. The system has been represented with a MIMO state space model. These have proven to be a useful representation that allow to represent complex systems and provide useful information for the state of the system at all time. Once observability and controllability of the system has been checked, a feedback controller with integration of the control error has been implemented using pole placement proving good results in the system output.

To study the Windup phenomenon, first, saturation effects in the output of the system have been analysed. References are reached but undesired behaviour emerges. Secondly, actuators have been limited even more and step references have been increased. In this situation, Windup materializes. The output cannot reach the reference due to the actuators' constraints and oscillations and delays in the response emerge. To avoid Windup, instead of designing a new controller, a modification to the feedback controller already implemented has been done. Based in the paper written by Kapoor, Teel and Daoutidis [17] a term containing an observer gain matrix has been added to the closed loop state equation. Two different methods have been implemented to obtain the observer gain matrix. One, using the algorithm described in [17] and another using pole placement. Both have shown very similar and satisfying results.

To conclude, this thesis has shown an efficient implementation of two Anti-Windup methods for LTI-MIMO systems. However, more research needs to be done in this field. New approaches are being developed, but a unified, robust, universal Anti-Windup procedure has not been achieved yet.

REFERENCES

- [1] Sergio Galeani, Sophie Tarbouriech, Matthew Turner and Luca Zaccarian. “A Tutorial on Modern Anti-windup Design” European Journal of Control. 2009.
- [2] Matlab Tech Talks. Understanding PID Control, Part 2: Expanding Beyond a Simple Integral. Obtained in the webpage: <https://www.mathworks.com/videos/understanding-pid-control-part-2-expanding-beyond-a-simple-integral-1528310418260.html>
- [3] Lecture Notes from the MIT Open Courseware. Topic #23 16.30/31 Feedback Control Systems. Obtained in the webpage: https://ocw.mit.edu/courses/aeronautics-and-astronautics/16-30-feedback-control-systems-fall-2010/lecture-notes/MIT16_30F10_lec23.pdf
- [4] Karl Johan Åström. “Control System Design. Lecture Notes for ME 155A”. Department of Mechanical and Environmental Engineering. University of California. Santa Barbara.
- [5] J.M. Gomes da Silva, S. Tarbouriech. “Anti-windup design with guaranteed regions of stability for discrete-time linear systems” System and Control letters 184-192. 2006.
- [6] S. Tarbouriech, M. Turner. “Anti-windup design: an overview of some recent advances and open problems” IET Control Theory and Applications. 2008.
- [7] Priv. Doz. Dr. Christoph Hametner, Univ. Prof. Dr. Stefan Jakubek and Sebastian Thormann Lecture notes. Zustandsregelung von Mehrgrößensystemen, English version Technical University of Vienna. 2009.
- [8] Matlab documentation. Obtained in the webpage: <https://www.mathworks.com/help/ident/ug/what-are-state-space-models.html#:~:text=State%2Dspace%20models%20are%20models,order%20differential%20o%20difference%20equations.>
- [9] Derek Rowell. “Analysis and Design of Feedback Control Systems State-Space Representation of LTI Systems”. 2002. Obtained in the webpage: <http://web.mit.edu/2.14/www/Handouts/StateSpace.pdf>
- [10] Radek Pelánek. “Properties of state spaces and their applications” Int J Softw Tools Technol Transfer. 10:443–454. 2008.
- [11] Three-tank figure. Obtained in the webpage: <https://www.google.com/url?sa=i&url=https%3A%2F%2Fwww.computer.org%2Fcsdl%2Fmagazine%2Fcs%2F2008%2F04%2Fmcs2008040050%2F13rUypGGeG&psig=AOvVaw2t3an9neqqwHQwsNCW4gma&ust=1595350326053000&source=images&cd=vfe&ved=0CAIQjRxqFwoTCMlail3OoCFQAAAAAdAAAAABAD>
- [12] Andrew J. Whalen, Sean N. Brennan, Timothy D. Sauer and Steven J. Schiff. “Observability and Controllability of Nonlinear Networks: The Role of Symmetry” Physical Review X. 5, 011005. 2015.
- [13] Goodwin, Graebe, Salgado. Chapter 17. Linear State Space Models. Prentice Hall. 2000. Obtained in the webpage: https://csd.newcastle.edu.au/book_slds_download/Ch17c.pdf

- [14] Brian Douglas. Matlab Tech Talks. State Space, Part 3: A Conceptual Approach to Controllability and Observability. Obtained in the webpage:
<https://www.mathworks.com/videos/state-space-part-3-a-conceptual-approach-to-controllability-and-observability-1548327460100.html>
- [15] Brian Douglas. Matlab Tech Talks. State Space, Part 2: Pole Placement. Obtained in the webpage:
<https://www.mathworks.com/videos/state-space-part-2-pole-placement-1547198830727.html>
- [16] Trentelman H.L., Antsaklis P. "Observer-Based Control" Baillieul J., Samad T. (eds) Encyclopedia of Systems and Control. Springer, London. 2014.
- [17] Navneet Kapoor, Andrew R. Teel and Prodrimos Daoutidis. "An Anti-Windup Design for Linear Systems with Input Saturation" Automatica Vol. 34, No 5, pp. 559-574. 1998.
- [18] Mayuresh V. Kothare, Peter J. Campo, Manfred Morari and Carl N. Nett. "A Unified Framework for the Study of Anti-windup Designs" Automatica Vol. 30, No. 12 pp. 1869-1883. 1994.
- [19] M. Zha, H. He and K. Ju, "Anti-windup based state feedback controller design for constrained T-S systems," 2019 Chinese Control Conference (CCC), Guangzhou, China, pp. 1214-1218. 2009.
- [20] Kaizhong Ju, Hanlin He and Miao Zha, "One step anti-windup based state feedback controller design for constrained T-S systems", 37th Chinese Control Conference. 2018.
- [21] X. Mo and Z. Li, "New Anti-windup Scheme for Linear Systems with Actuator Saturation," 2019 3rd International Conference on Robotics and Automation Sciences (ICRAS), Wuhan, China, pp. 96-101, 2009.
- [22] Zhang, Dai & Li, Hui & Collins, Emmanuel." Digital Anti-Windup PI Controllers for Variable-Speed Motor Drives Using FPGA and Stochastic Theory". Power Electronics, IEEE Transactions. 2006.